

**THE LENGTHENING OF THE AMAZON DRY SEASON:  
INFLUENCE ON WATER VAPOR TRANSPORT TOWARD THE INTRA-  
AMERICAN REGION**

Master Student:  
JHOANA AGUDELO RENDÓN

Advisors:  
PAOLA ANDREA ARIAS GÓMEZ  
SARA CRISTINA VIEIRA AGUDELO

Grupo de Investigación y Gestión Ambiental (GIGA)  
Escuela Ambiental, Facultad de Ingeniería  
Universidad de Antioquia

April 2017

## Abstract

Several studies have identified a lengthening of the dry season over the southern Amazon during the last three decades. Some explanations to this lengthening suggest the influence of changes in the regional circulation over the Atlantic and Pacific oceans, whereas others point to the influence of vegetation changes over the Amazon rainforest. This study aims to understand the implications of more frequent long dry seasons in this forest on atmospheric moisture transport toward northern South America and the Caribbean region. Using a semi-Lagrangian model for water vapor tracking, results indicate that longer dry seasons in the Amazon relate to reductions of water vapor content over the southern and eastern Amazon basin, due to significant reductions of evaporation and recycled precipitation rates in these regions, especially during the transition from dry to wet conditions in the Amazon. On the other hand, longer dry seasons also relate to enhanced atmospheric moisture content over the Caribbean and northern South America regions, mainly due to increased contributions of water vapor from oceanic regions and the increase of surface moisture convergence over the equatorial region. This highlights the importance of understanding the relative role of regional circulation and local surface conditions on modulating water vapor transport toward continental and oceanic regions.

**Keywords:** Water vapor transport, northern South America, Amazon dry season, water vapor tracking.

## 1. Introduction

Climate and eco-hydrological conditions over the Amazon, the largest tropical rainforest on the planet (Foley et al. 2007), are matter of increasing interest in the scientific community. This tropical rainforest offers multiple benefits and ecological services, not only to the region but also to the entire planet, since it plays an important role on the global hydrological and energetic balance (Drumond et al. 2014). Because of the huge amounts of local evapotranspiration, the Amazon basin constitutes an important atmospheric humidity reservoir for the region. Several studies have identified that the Amazon climate represents an important element for the hydro-climatology of northern South America, because considerable amounts of moisture that evaporates from the rainforest is transported by the atmospheric circulation northwards, contributing to trigger precipitation over the north of the continent (Yin et al. 2014; Juárez et al. 2007). Nevertheless, the rapid development of the agricultural frontier of the Amazon, especially in the Brazilian Cerrado, has increased the vulnerability of this rainforest and surrounding areas regarding to climate change (Sampaio et al. 2007; Soares-Filho et al. 2006; Morton et al. 2006). A manifestation of such vulnerability corresponds to the strong drought events reported in 2005 and 2010 in this forest (Davidson et al. 2012).

The vulnerability of the Amazon and the eco-hydrological services provided by this forest depend on an adequate moisture supply (as precipitation or moisture stored in the soil) during its dry season and transition to the wet season (Boisier et al. 2015). The transition from the dry to the wet season obeys mainly to the activation of the South American monsoon system (SAMS), largely controlled by large-scale thermodynamic processes, such as variations of the equatorial sea surface temperature (SST) (e.g., Marengo et al. 2001; Liebmann and Marengo 2001; Carvalho et al. 2011). In particular, the onset of the Amazon wet season emerges from the contribution of three main elements: increases of local evapotranspiration, synoptic disturbances such as cold air incursions, and large-scale moisture transport from surrounding oceans (Li and Fu 2004; Fu and Li 2004; Yin et al. 2014).

Recent studies report a lengthening of the dry season over the southern Amazon during the last few decades, consistent with a more frequent occurrence of shorter wet seasons in the region, a reduction of precipitation rates, and an expansion of the savanna ecosystem in this forest (Fu et al. 2013; Debortoli et al. 2015). The latter leads to a loss of soil absorption and carbon reservoir capacity in the Amazon (Boisier et al. 2015). The strongest changes related to a lengthening of the dry season in this forest occur during the dry-to-wet transition season (which occurs from September to November - SON), and are closely associated with local changes in land cover (Fu and Li 2004; Costa and Pires 2010). Thus, several studies addressing the recent variations on the Amazon dry season and its transition to the wet period focus on local surface processes (related to albedo, roughness, soil temperature), and large-scale atmospheric dynamics (Oyama and Nobre 2003; Sampaio et al. 2007; Sampaio 2008; Salazar and Nobre 2010). However, other studies suggest that this lengthening also relates to an alteration of regional circulation patterns due to a thermodynamic response to SST changes in the surrounding oceans that induce local conditions to become increasingly dryer over the

Amazon and enhance water vapor transport toward northern South America (**Arias et al. 2015a**). In particular, longer dry seasons in the Amazon (related to a shorter South American Monsoon) are characterized by enhanced atmospheric moisture transport and convection over the South American equatorial region, mainly during the transition from the North American monsoon system (NAMS) to the SAMS (which occurs during SON), induced by stronger Hadley and Walker regional cells. As a result, larger convection over the equatorial region during this inter-hemispheric transition between monsoons would inhibit precipitation over the Amazon, inducing a lengthening of its dry season (**Arias et al. 2015a**). Therefore, this paper aims at establishing whether there has been an increase of water vapor transport toward northern South America in association with longer dry seasons over the Amazon rainforest throughout the last decades. A semi-Lagrangian model for tracking water vapor is used to determine the main sources contributing to this transport.

This paper is divided as follows: data and methodology are presented in section 2, including a brief description of the model used to track water vapor over the equatorial Americas and the Intra-American sea (IAS) region; section 3 presents the main results; finally, section 4 includes the discussion and main conclusions from this study.

## 2. Data and Methods

To analyze the influence of the Amazon dry season lengthening on atmospheric moisture transport toward northern South America and the IAS region, this study focuses on the analysis of atmospheric variables and water vapor transport estimates during years with long and short dry seasons in the Amazon (hereafter LDS and SDS, respectively), according to the classification criterion presented in section 2.2. To estimate statistical significance in the difference of composites of atmospheric moisture transport during LDS and SDS cases, a bootstrap test is used. We consider a 95% confidence level in the statistical test.

We use monthly zonal, meridional, and vertical winds ( $u$ ,  $v$ , and  $w$ , respectively) from the European Centre for Medium-Range Weather Forecast reanalysis (ECMWF) ERA-Interim (**Dee et al. 2011**) for the period 1980-2010, at a spatial resolution of  $0.75^\circ$ . We use ERA-Interim reanalysis due to its better representation of the hydrological cycle and atmospheric moisture transport (**Dee et al. 2011; Trenberth et al. 2011**).

We also used four databases for precipitation: the National Oceanic and Atmospheric Administration (NOAA) Climate Diagnostics Center (CDC) daily precipitation gridded data version SA24 ( $1.0^\circ \times 1.0^\circ$  lat lon), available from January 1940 to December 2011 (**Liebmann and Allured 2005**); the Global Precipitation Climatology Project (GPCP) version 2.3, with monthly precipitation during the period 1979-present at a  $2.5^\circ \times 2.5^\circ$  horizontal grid (**Adler et al. 2003**); the Climate Prediction Center (CPC) Merged Analysis of Precipitation (CMAP) dataset with monthly precipitation during the period 1979-present and a  $2.5^\circ$ -horizontal grid (**Xie and Arkin 1997**); and the Precipitation Estimation from Remotely Sensed Information using Artificial Neural Networks (PERSIANN) dataset, which provides daily rainfall estimates at a spatial resolution of  $0.25^\circ$  in the latitude band  $60^\circ\text{S} - 60^\circ\text{N}$  from 1983 to the near-present (**Ashouri et al. 2015**).

In addition, as a qualitative index for vegetation cover in the Amazon, we use Leaf Area Index (LAI) dataset produced by the Centre National de Recherches Météorologiques (CNRM), as part of the earth2Observe Project, which provides monthly LAI measurements available during the period 1979-2012 at a  $1.0^\circ \times 1.0^\circ$  horizontal grid (**Schellekens et al. 2015**).

We compute SST anomalies over the tropical north Atlantic (TNA) as the domain average in the region  $60^\circ - 30^\circ\text{W}$ ,  $5^\circ\text{N} - 25^\circ\text{N}$ , using the monthly dataset provided by ERA Interim reanalysis (**Dee et al. 2011**) for the period 1980-2010 and a spatial resolution of  $0.75^\circ$ .

### 2.1 Hadley and Walker cells

The regional Hadley Cell is evaluated using the meridional mass streamfunction ( $\Psi$ ) calculated from the irrotational (or divergent) component of the meridional flow, as proposed by **Zhang and Wang (2013)**. The computation involves the irrotational components of the zonal mean meridional wind ( $v_{IR}$ ) over the South American sector ( $70^\circ\text{W} - 50^\circ\text{W}$ ,  $15^\circ\text{S} - 10^\circ\text{N}$ ). Here,  $\Psi$  is defined as the vertically integrated northward mass flux at latitude  $\phi$  from pressure level  $p$  to the top of the atmosphere. Thus,

$$\Psi(\phi, p) = \frac{2\pi \cos \phi}{g} \int_0^p [v_{IR}(\phi, p)] dp \quad (1)$$

where  $g$  denotes the acceleration due to gravity. All the calculations are carried out from monthly mean values obtained from ERA-Interim reanalysis, from which climatological means are calculated, and seasonal and annual means evaluated.

On the other hand, the regional Walker cell is studied from the analysis of vertical cross-sections for regional zonal divergent circulation over South America, where the divergent zonal wind component and the vertical velocity are averaged over the 15°S-5°S and equator-10°N latitudinal belts, for the longitudinal section between 140°W and 10°W.

## 2.2 Domain for water vapor tracking

To estimate the atmospheric moisture transport over the Intra-American region, we use the “Dynamic Recycling Model (DRM)”. In its original version, the DRM is a model for estimating precipitation recycling (**Domínguez et al. 2006**). The DRM is an analytical model formally derived from the equation of mass conservation. The model is formulated under a Lagrangian framework in which the storage variable is not negligible, allowing the analysis on a wide range of time scales (daily time scale included) of recycled moisture, its temporal and spatial variations, its main contributors, and its propagation toward different regions. The DRM is derived from the vertical integrated water vapor balance equation (see e.g. **Burke and Zangvil 2001**):

$$\frac{\partial(W)}{\partial t} + \frac{\partial(WU)}{\partial x} + \frac{\partial(WV)}{\partial y} = E - P \quad (2)$$

With:

$$W = \int_0^{p_0} \bar{q} \frac{dp}{g}$$

$$U = \frac{1}{W} \int_0^{p_0} \bar{q} \bar{u} \frac{dp}{g} + \int_0^{p_0} \overline{q' u'} \frac{dp}{g}$$

$$V = \frac{1}{W} \int_0^{p_0} \bar{q} \bar{v} \frac{dp}{g} + \int_0^{p_0} \overline{q' v'} \frac{dp}{g}$$

Where  $u$ ,  $v$  and  $w$  are zonal, meridional and vertical wind components, respectively,  $E$  is evaporation,  $P$  is precipitation,  $W$  is precipitable water, and  $q$  is specific humidity, where all variables are monthly means.  $U$  and  $V$  are effective zonal and meridional wind components.

**Domínguez et al. (2006)** found that, using the well-mixed atmosphere assumption, the fraction of moisture collected by an air column along its trajectory (given by the effective wind ( $U, V$ )) between times 0 and  $\tau$  is given by

$$R(\chi, \xi, \tau) = 1 - \exp \left[ - \int_0^\tau \frac{E(\chi, \xi, \tau)}{W(\chi, \xi, \tau)} \partial \tau' \right]$$

With:

$$\chi = x - ut$$

$$\xi = y - ut$$

$$\tau = t$$

This expression is a nonlinear function of the trajectory. **Martínez and Domínguez (2014)** found an analytical decomposition that allows to distinguish the contributions from different parts of the trajectory. This information can be used to estimate not only water vapor/precipitation recycling (i.e. the contribution of a region to its own moisture budget) but also the contributions from different regions to a given target region.

Since the DRM is a 2D model, its approach has been debated because vertical wind shear can induce patterns of moisture transport that are not quantified in the vertically integrated water flux (**Goessling and Reick 2013; Van der Ent et al. 2013**). However, the DRM can still provide valuable information when used in conjunction with more traditional methods, including detailed analyses of the wind patterns, both horizontally and vertically. This has been the approach in previous studies using the DRM, like **Martínez and Domínguez (2014)**, **Arias et al. (2015b)** and **Pathak et al. (2016)**. Moreover, **Hoyos et al. (2017)** compare the DRM to other water accounting models for the same region of this study, finding reasonable agreement between the DRM and the Quasi-Isentropic Back Trajectory (QIBT) model (**Dirmeyer et al. 2009**) (**Goessling and Reick 2013; Van der Ent et al. 2013; Pathak et al. 2017; Hoyos et al. 2017; Dirmeyer et al. 2009**).

In this study, we use the DRM for tracking atmospheric moisture in the domain and between the regions shown in Figure 1. This domain includes Central America and a fraction of North and South America. The continental regions are subdivided into 13 subregions while the adjacent oceans are subdivided into 8 subregions. We consider the latest DRM version presented by **Martínez and Domínguez (2014)**, using daily data from ERA-Interim for precipitation, evaporation, and precipitable water (P, E, and W, respectively), and daily data of vertically integrated water vapor flux for both zonal (**U**) and meridional (**V**) directions.

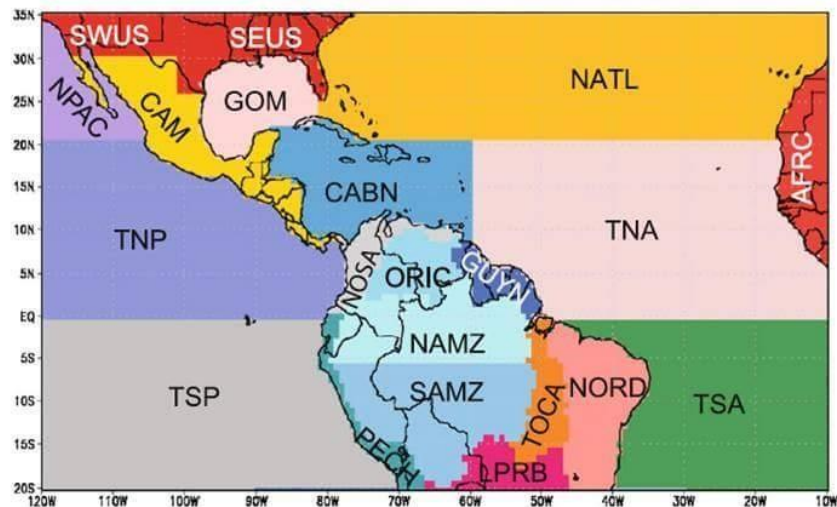


**Figure 1.** Domain used to implement the DRM to estimate atmospheric moisture transport from and toward different regions in the Intra-American region. The domain is subdivided into 21 subregions: *NOSA* Northern South America domain, *NPAC* Northern Pacific, *TNP* Tropical North Pacific, *TSP* Tropical South Pacific, *NATL* North Atlantic, *TNA* Tropical North Atlantic, *TSA* Tropical South Atlantic, *CAM* Central America and Mexico, *GOM* Gulf of Mexico, *CABN* Caribbean Sea, *ORIC* Orinoco Region, *GUYN* Guyanas, *PECH* Peru–Chile, *NAMZ* Northern Amazon, *SAMZ* Southern Amazon, *TOCA* Tocantins river, *NORD* Brazil’s Northeast, *LPRB* La Plata River Basin, *AFRC* Africa, *SEUS* South Eastern United States, *SWUS* South Western United States.

### 2.3 Amazon dry season length

As pointed out in the Introduction, previous studies have identified a recent lengthening of the dry season in the Amazon forest during the past few decades (**Fu et al. 2013; Debortoli et al. 2015**). This paper is focused on analyzing the effects of such lengthening on the atmospheric moisture transport over the Intra-American region by comparing moisture transport processes between the years with the longest and the shortest dry seasons in Amazon rainforest occurred between 1980 and 2010.

The dry season length is computed for each year as the difference between the date corresponding to the wet season onset and the date corresponding to the wet season retreat in the southern Amazon, expressed in pentads (i.e., five-days average; see e.g., **Fu et al. 2013**). Following **Li and Fu (2004)**, the wet season onset/retreat dates are obtained considering both an objectively-defined rain rate threshold and the persistence in time. Thus, the wet season onset (retreat) date is defined as the pentad before which the rain rate is less (more) than the climatological annual mean rain rate during 6 out of 8 preceding pentads and after which the rain rate is greater (lower) than the climatological annual mean rain rate during 6 out of 8 subsequent pentads. This criterion has been widely applied in previous studies regarding monsoonal systems (**Kousky 1988; Li and Fu 2004; Fu and Li 2004; Arias et al. 2012, 2015a; Fu et al. 2013**). To obtain wet season onset/retreat, we consider SA24 daily precipitation data for the region from 50°W to 70°W and 15°S to 5°S, corresponding to the southern Amazon.

Finally, each year within the period of study is classified into one out-of-three categories, corresponding to years with a dry season: (1) longer than 75% of one standard deviation ( $0.75\sigma$ ) above the climatological length (LDS), (2) shorter than  $0.75\sigma$  below the climatological length (SDS), and (3) within a range between the climatological length minus/plus  $0.75\sigma$  (normal dry seasons) (Figure 2). Table 1 shows the years of LDS and SDS obtained with this method. Notice that the longest dry seasons (LDS) are more frequent since the 90s, while the shortest dry seasons (SDS) are more frequent during the 80s. The latter is in agreement with previous studies that identify a trend toward longer dry seasons in the southern Amazon during the past two decades (**Fu et al. 2013; Debortoli et al. 2015**).

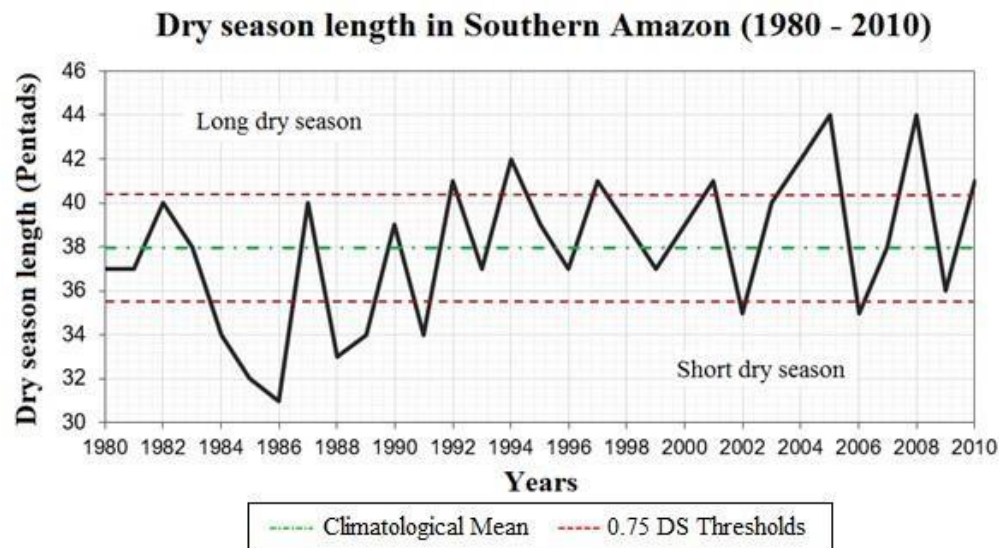


**Figure 2.** Length of the dry season in the southern Amazon during the period 1980-2010 obtained from SA24 data. Years are classified into long (LDS), short (SDS), and normal dry seasons.

**Table 1.** Years with the longest (LDS) and the shortest (SDS) dry seasons in the Amazon during the period 1980- 2010. \* indicates El Niño years. \*\* indicates La Niña years.

LDS	SDS
1992	1984
1994	1985
1997*	1986
2001	1989
2004	1991
2005	2002*
2008	2006*
2010**	



### 3. Results

#### 3.1 Water vapor contributions toward northern South America during LDS and SDS

In order to identify the regions with the largest contributions of atmospheric moisture to northern South America and the Caribbean during LDS and SDS events, we composite the precipitable water transported from each source depicted in Figure 1 to northwestern South America (NOSA), the Orinoco basin (ORIC), and the northern Amazon (NAMZ) domains, during LDS and SDS years (Table 1). Precipitable water contributions are calculated with the DRM. Figures 3 to 5 show the mean annual cycle of precipitable water transported to the continental regions in northern South America (NOSA, ORIC, NAMZ) from the sources located in the Caribbean Sea and Atlantic Ocean, the Pacific Ocean, and northern South America, respectively, during LDS and SDS years. **Arias et al. (2015b)** discuss a more detailed analysis of the climatological contributions from these regions; here we focus on the differences between LDS and SDS events.

Figure 3a shows that one of the most important sources of atmospheric moisture toward northern South America is the northern tropical Atlantic Ocean region (TNA), exhibiting the largest contributions to NOSA, ORIC, and NAMZ throughout the year, especially during December to February (DJF) and March to May (MAM) seasons. There are also important contributions from the tropical region of the South Atlantic Ocean (TSA) toward the northern Amazon region (NAMZ), mainly during austral winter (June to August – JJA). These contributions occur during both LDS and SDS years, although the differences between both types of dry seasons are not statistically significant. On the other hand, Figure 3b shows that the moisture contributions from NATL and CABN are lower than from the TNA and TSA sources. The largest contribution from the Caribbean is to northwestern South America (NOSA) during DJF, mainly during LDS events. The contribution from the Caribbean to the rest of South America is negligible when compared with the other sources.

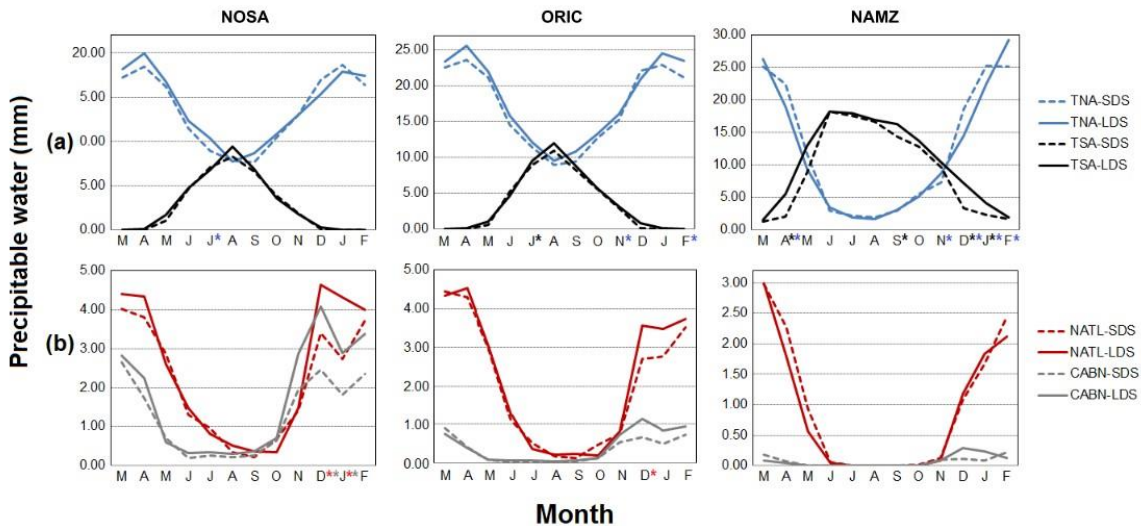


**Figure 3.** Annual cycle of precipitable water (mm) transported to NOSA, ORIC, and NAMZ during LDS and SDS from (a) TNA and TSA sources, and (b) NATL and CABN sources. The asterisk located in the upper right corner in some months (horizontal axis) indicates statistically significant differences between LDS and SDS events, according to a Bootstrap test.

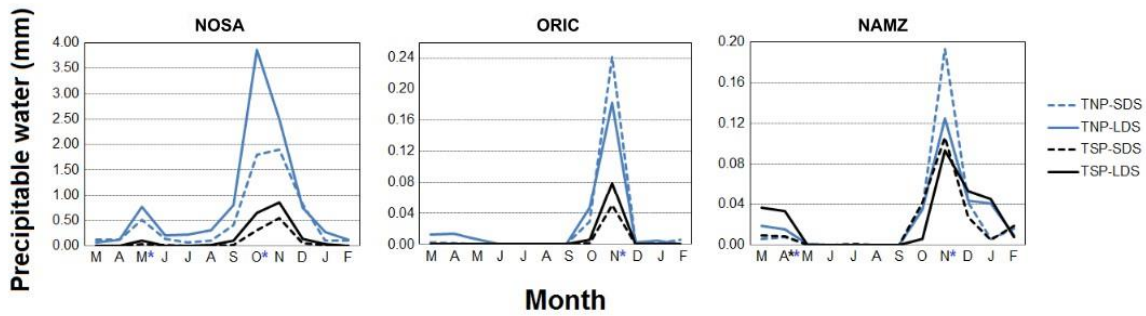


Figure 4. Same as Figure 3 but from TNP and TSP sources.

Regarding the Pacific Ocean sources, Figure 4 shows that the tropical North Pacific Ocean (TNP) is the region with largest contributions to northern South America compared to the tropical south Pacific (TSP), for both LDS and SDS events. However, LDS events are associated with larger moisture contributions from TNP to NOSA while the occurrence of these events reduces moisture transport to ORIC and NAMZ regions. These changes appear to be important, especially during the transition from dry to wet conditions in the Amazon (SON season). Contributions from the north Pacific (NPAC) region are not shown since there are not significant contributions from this region to the three sink regions considered (NOSA, ORIC, and NAMZ).

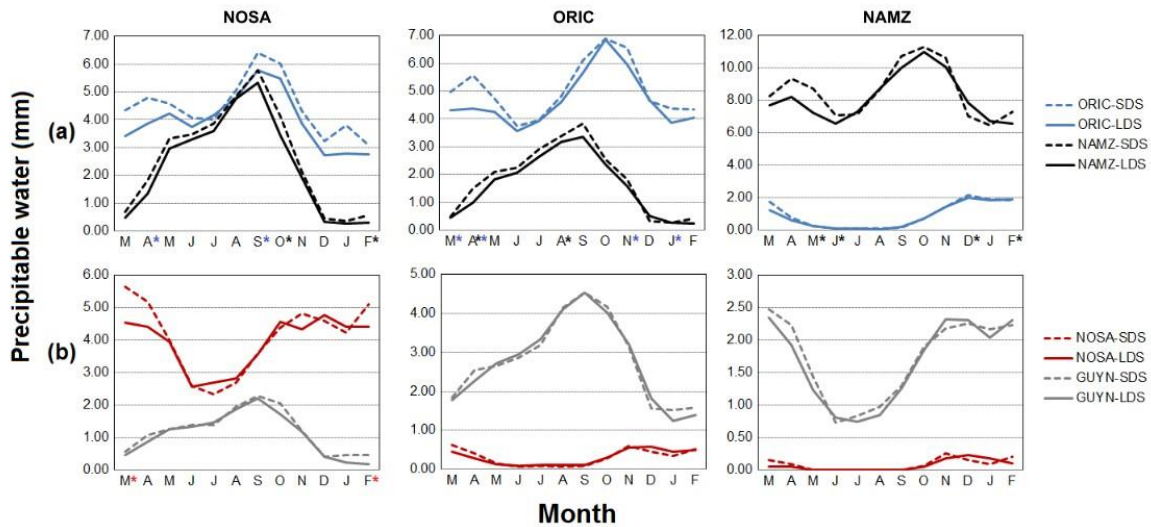


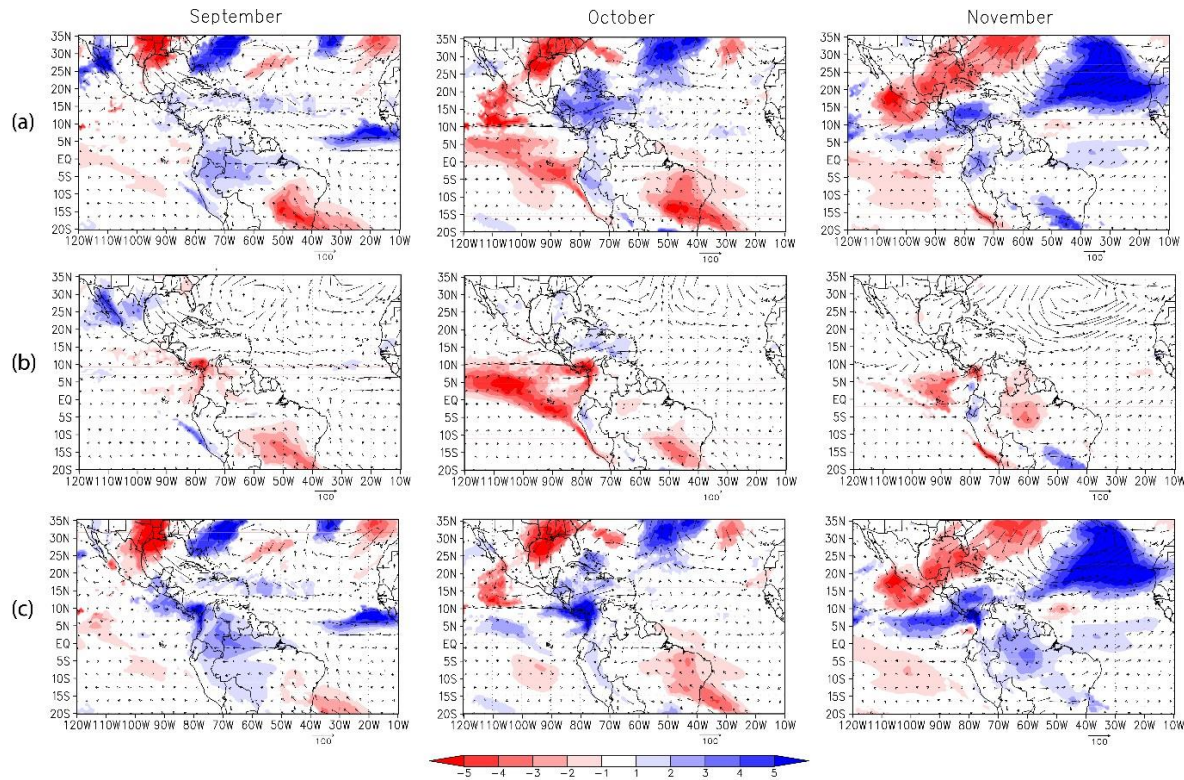
Figure 5. Same as Figure 3 but from (a) ORIC and NAMZ sources, and (b) NOSA and GUYN sources.

Finally, Figure 5a highlights the dominant role of recycled precipitation for the Orinoco basin (ORIC) and northern Amazonia (NAMZ), since the main contributions of atmospheric moisture to these regions come from their own domain (only exceeded by contributions from TNA in DJF and MAM). Thus, precipitation and recycled moisture in these regions exceed in magnitude the contributions of advected water vapor from surrounding continental (Figure 5b) and oceanic regions (Figures 3 and 4). By contrast, although local precipitation recycling plays an important role in northwestern South America (northwestern Colombia and northern Venezuela - NOSA), advection from other continental sources like the Orinoco basin and the northern Amazon during austral winter (JJA), as well as from oceanic sources like the TNA during MAM, exhibits the largest magnitudes. These contributions occur for both LDS and SDS events.



### 3.2 Effects on regional atmospheric moisture transport

To identify the spatial distribution of atmospheric moisture content in the Intra-American region during LDS and SDS events in the Amazon, we estimate total precipitable water contributions from continental-only, oceanic-only, and all sources (continental + oceanic) presented in Figure 1. We make composites of LDS and SDS years in the period 1980-2010, estimating the difference between both cases (LDS-SDS). Thus, positive (negative) differences indicate enhanced (reduced) moisture transport at each specific location from the corresponding source (i.e. continental, oceanic, all sources) during LDS events.



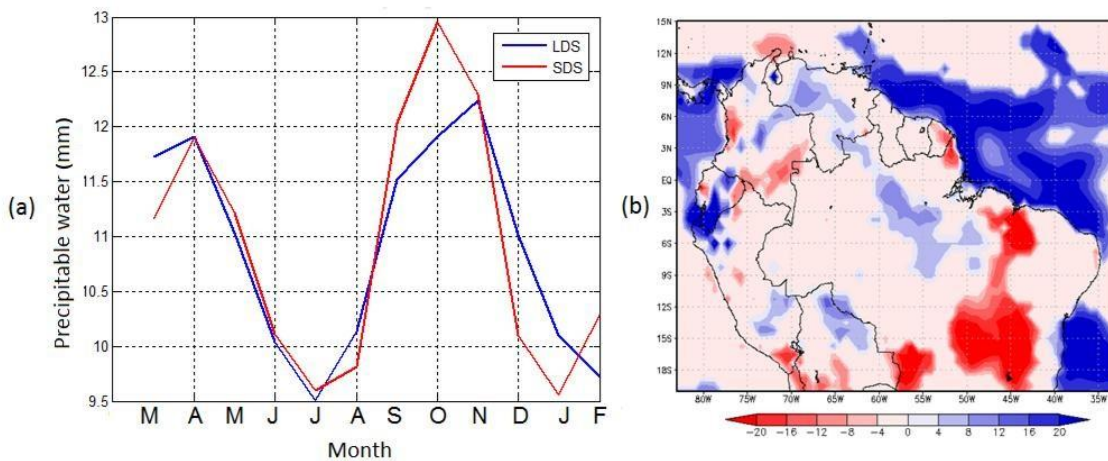
**Figure 6.** Differences between LDS and SDS years for precipitable water [mm] from DRM (shaded) transported from (a) all, (b) continental-only and (c) oceanic-only water vapor sources presented in Figure 1, during the dry-to-wet transition period in the Amazon (SON). Vectors indicate the Vertical Integrated Moisture Flux (VIMF) differences [kg/ms] using ERA-Interim (vectors). Only significant differences according to a bootstrap test are shown.

Figure 6 shows the difference in contributions between LDS and SDS composites during the dry-to-wet transition season in the Amazon (SON). Results indicate that during the occurrence of LDS years, significant reductions of atmospheric moisture occur especially over the south and southeastern Amazon during the first two months of the transition period (Figure 6a). For example, Figure 6a for September shows that the combined contribution from the sources in Figure 1 to the precipitable water over the southeastern Amazon basin is nearly 4 mm less during LDS than during SDS events. These reductions are associated with reductions in water vapor transport from continental sources (Figure 6b), especially from less precipitation recycled in the southern Amazon (SAMZ), rather than from oceanic moisture (Figure 6c). The latter is better observed in Figure 7a, which shows that the occurrence of LDS events in the Amazon is associated with important reductions on atmospheric moisture originated from the southern Amazon (SAMZ), especially during the first two months of the dry-to-wet transition season. Thus, a strong reduction of precipitation recycling to the south of the Amazon is the process that contributes the most to the reductions of atmospheric moisture content observed in this region during the LDS events (Figure 6a). Furthermore, Evapotranspiration (ET) is reduced over the southern Amazon (according to ERA-Interim) during LDS years (Figure 7b), in agreement with the reduced precipitation recycling suggested by the DRM.

Another important feature in Figure 6 is the increase of atmospheric moisture over northern South America and the Caribbean Sea observed during LDS events (Figure 6a). Such an increase is related to enhanced contributions of atmospheric moisture coming from the oceanic regions (Figure 6c) rather than from continental sources (Figure 6b).

The reductions of atmospheric moisture over the Amazon and the increases over northern South America and the Caribbean Sea during LDS events estimated by the DRM are in agreement with precipitation changes depicted by observational data (Figure 8). Moreover, the pattern observed in Figure 8 resembles the changes of precipitation reported by **Arias et al. (2015a)** when considering long transition seasons from the NAMS to the SAMS, which correspond to the transition season from dry to wet conditions in the Amazon (SON). Figures 6 to 8 provide further evidence regarding the possible influence of a lengthening of the Amazon dry season at regional scale, since they indicate that atmospheric moisture reductions in the Amazon are related to local processes such as precipitation recycling whereas water vapor increases in the equatorial Americas and the Caribbean are related to the influence of oceanic sources.

An important feature found on the VIMF anomalies is that during the occurrence of LDS years in the Amazon, the trade winds magnitude decreases throughout the transition period from dry to wet conditions (e.g. Figure 6). Also, notice the significant enhancement of the westerly water vapor transport over the eastern tropical Pacific Ocean toward western Colombia, observed during LDS events, mainly in October and November. This westerly flux is mainly associated with the Choco low-level jet (**Poveda and Mesa 2000; Poveda et al. 2014**), an important climate feature over the region which exhibits its largest intensities during October-November and is partially related to the inter-hemispheric SST gradient in the eastern Pacific (**Poveda and Mesa 2000; Sierra et al. 2017**).



**Figure 7.** (a) Annual cycle of moisture recycling in the southern Amazon (SAMZ) during LDS (blue line) and SDS (red line) years. (b) Evaporation differences [in mm/month] between LDS and SDS years (LDS-SDS) during the transition period from dry to wet conditions in the Amazon (SON), according to ERA-Interim reanalysis data.



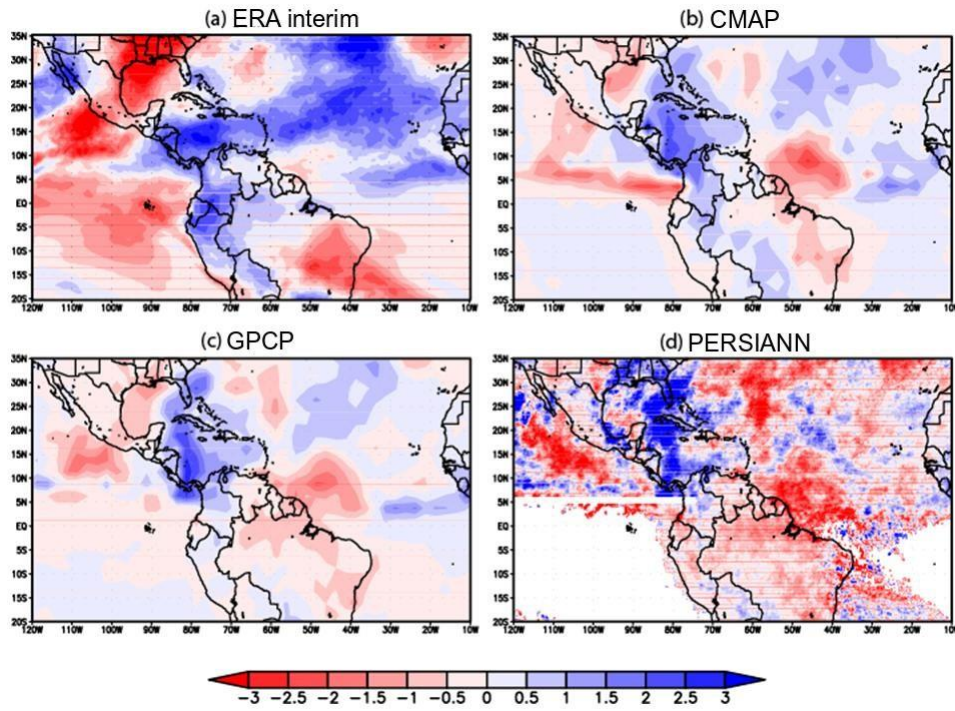


**Figure 8.** Precipitation differences between LDS and SDS years (LDS-SDS) during the transition period from dry to wet conditions in the Amazon (SON) for (a) ERA-Interim, (b) CMAP, (c) GPCP, and (d) PERSIANN datasets. Data in mm/day.

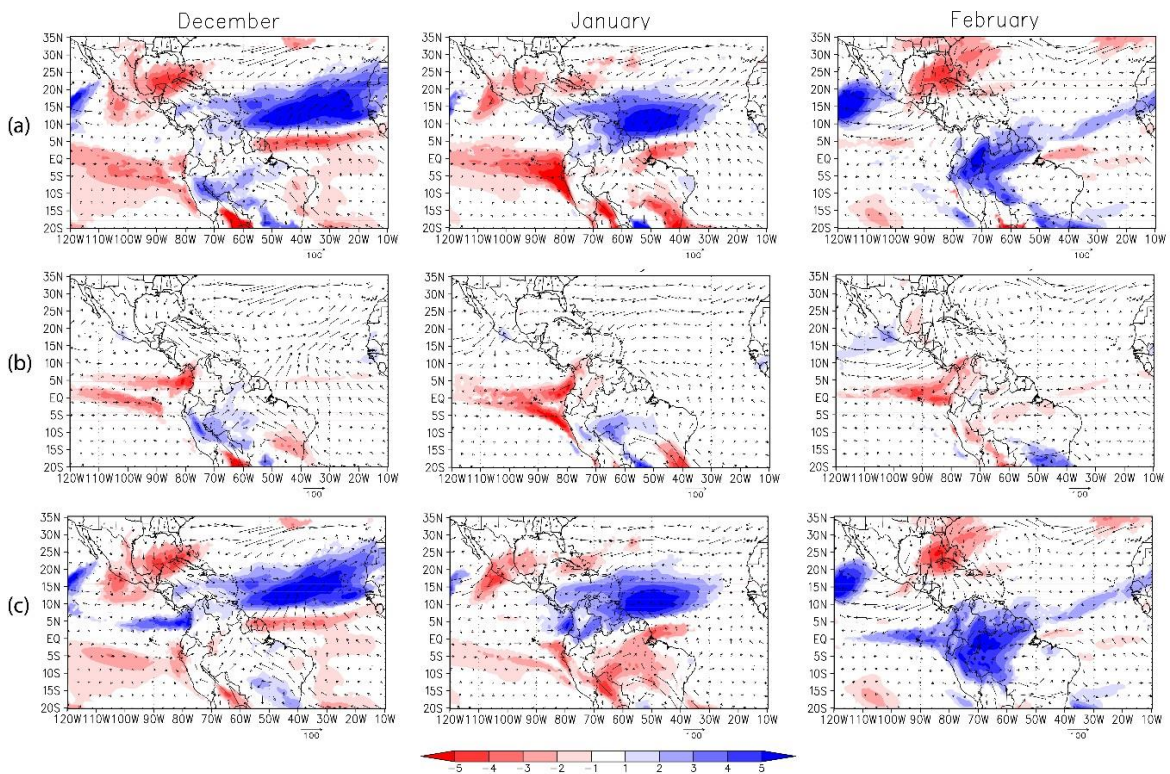


**Figure 9.** Same as Figure 6 but for DJF.

Figure 9 shows changes of atmospheric moisture contributions from continental, oceanic, and all sources between LDS and SDS events during the Amazon wet season (DJF). The largest differences are observed for the atmospheric moisture contributions originated over the oceans (Figure 9c), indicating a pattern of surface moisture convergence, especially over the tropical north Atlantic Ocean (TNA). This pattern of enhanced moisture in the TNA migrates southeasterly throughout the Amazon wet season, increasing moisture transport toward the Caribbean and northern South America during January and February, respectively. On the other hand, water vapor contributions originated over the continental landmass (Figure 9b) does not exhibit significant differences over northern South America and the Caribbean, although small reductions are observed over Colombia and the eastern tropical Pacific Ocean in the late wet season. When considering the atmospheric moisture originated from all the sources included in the domain (Figure 9a), a remarkable difference on the spatial distribution of moisture is observed, being strongly influenced by oceanic contributions.

### 3.3 Connections between Amazon LDS and the regional atmospheric circulation

**Arias et al. (2015a)** suggest that longer transition periods between NAMS and SAMS, partially associated with longer dry seasons in the Amazon, appear to relate to the enhancement of regional Walker and Hadley cells in South America. The composite analysis proposed by **Arias et al. (2015a)** is based on the length of the transition season between both monsoons rather than on the length of the Amazon dry season. Here, we analyze the regional Walker and Hadley cells during LDS and SDS events, in order to identify if a lengthening of the Amazon dry season could be linked to significant changes in these circulations in South America.

Figure 10 shows the mean vertical cross-sections of the regional meridional divergent circulation and mass streamfunction over South America during LDS and SDS events, and their difference, for both SON and DJF seasons. Upward motion is located at 5°S during the dry-to-wet transition season in the Amazon (SON) whereas this ascending branch migrates southward up to 10°S in austral summer (DJF), a feature dominated by the seasonal migration of the Intertropical Convergence Zone (ITCZ). This is observed during both LDS and SDS years; however, LDS events are characterized by anomalous ascending motion over the equatorial region during both seasons. Furthermore, subtropical South America shows an increase of downward motion during LDS years, especially in austral summer (Figure 10b). Regional meridional divergent circulation is consistent with the atmospheric moisture content patterns shown in Figures 6 and 9, where stronger surface divergence (convergence) is observed over the Amazon (equatorial Americas), with anomalous subsidence (ascending motion) over the region during LDS events in the Amazon. The latter is consistent with a stronger regional Hadley cell in association with a longer dry season in the Amazon.

Figures 11a and 11b show the regional Walker circulation for the Pacific-South America-Atlantic sector over the southern hemisphere (140°W-10°W, 15°S-5°S) during LDS and SDS years, and their difference, for SON and DJF, respectively. Ascending motion is located between the longitudes 80°W-40°W, which corresponds to South American landmass. On the other hand, descending motion occurs over the oceans, at longitudes between 140°W-80°W (Pacific Ocean) and 40°W-20°W (Atlantic Ocean). As expected, ascending motion in South America is stronger during austral summer (DJF; Figure 11b) due to the southward migration of the ITCZ, favoring surface convergence and strengthened ascending motion over this region. LDS years exhibit stronger upward motion over the Andes and western Amazon (80°W-60°W), and intensified subsidence over the eastern Amazonia (45°W-40°W). Similarly, when comparing LDS and SDS patterns during DJF, LDS years show a strengthening of the ascending motion over the western Amazon while the ascending motion weakens to the east of the Amazon basin.



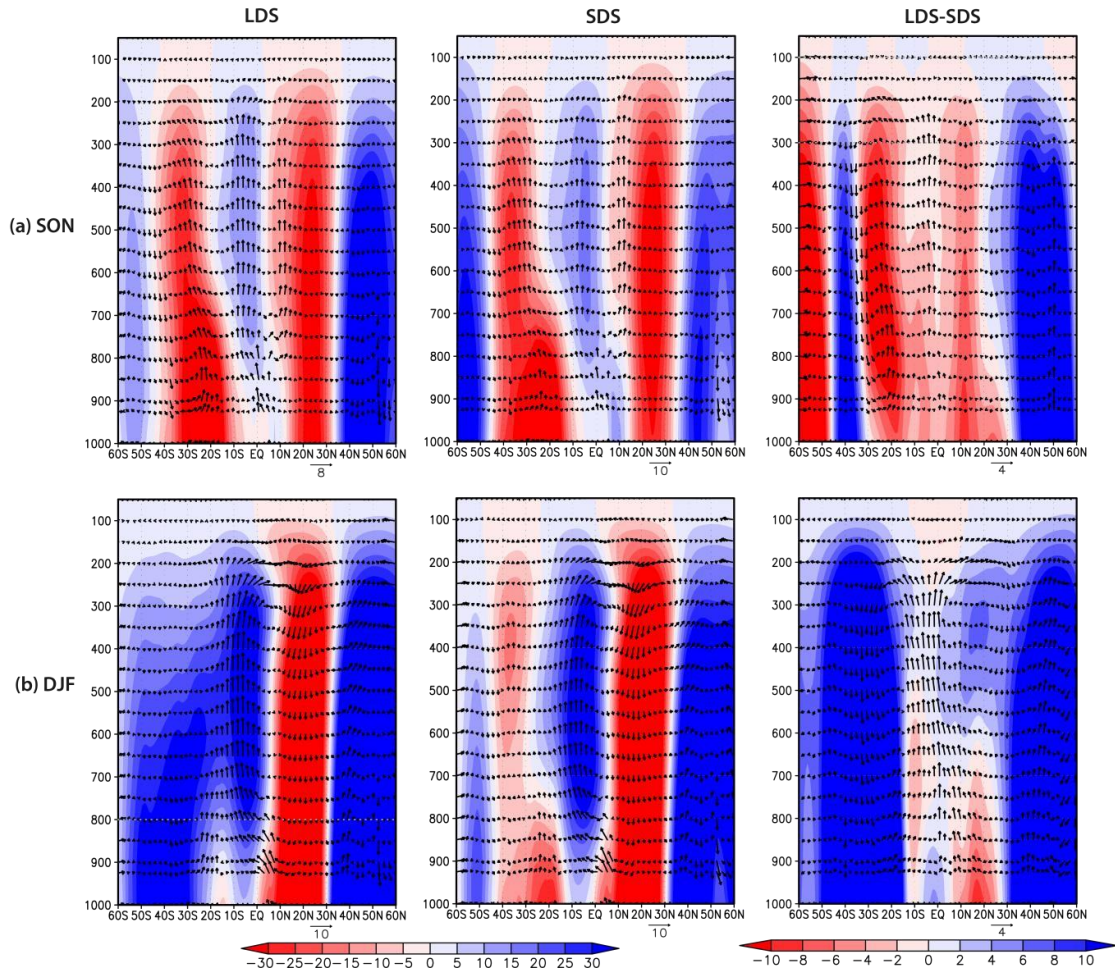


**Figure 10.** Vertical cross-sections for regional meridional mass streamfunction (shades) and meridional divergent circulation (vectors) over South America during LDS and SDS years, and their difference, for (a) SON and (b) DJF. Vectors are plotted as the divergent meridional wind component and the vertical velocity zonally averaged over the longitudes  $70^{\circ}\text{W}$ - $50^{\circ}\text{W}$ . The vector scale shown in the bottom right corner of each panel is multiplied by  $10^{-4} \text{ hPa s}^{-1}$ .

Figures 12a and 12b show the regional Walker circulation for the Pacific-South America-Atlantic sector over the northern hemisphere ( $140^{\circ}\text{W}$ - $10^{\circ}\text{W}$ ,  $0^{\circ}$ - $10^{\circ}\text{N}$ ) during LDS and SDS years, and their difference, for SON and DJF, respectively. Ascending motion is located near the  $80^{\circ}\text{W}$  longitude, which corresponds to the region between western Colombia and eastern Tropical North Pacific (TNP). Ascending motion in northern South America ( $0^{\circ}$ - $10^{\circ}\text{N}$ ) is stronger during the dry-to-wet Amazon transition season (SON; Figure 12a), since the ITCZ is located over this region during these months. LDS years exhibit stronger upward motion near  $80^{\circ}\text{W}$ . Similarly, when comparing LDS and SDS patterns during DJF, LDS years show a strengthening of the ascending motion over western northern South America. Thus, changes in both regional Hadley and Walker cells during LDS events are consistent with enhanced moisture transport and precipitation toward northern South America during SON and DEF, as depicted by Figures 6, 8, and 9.



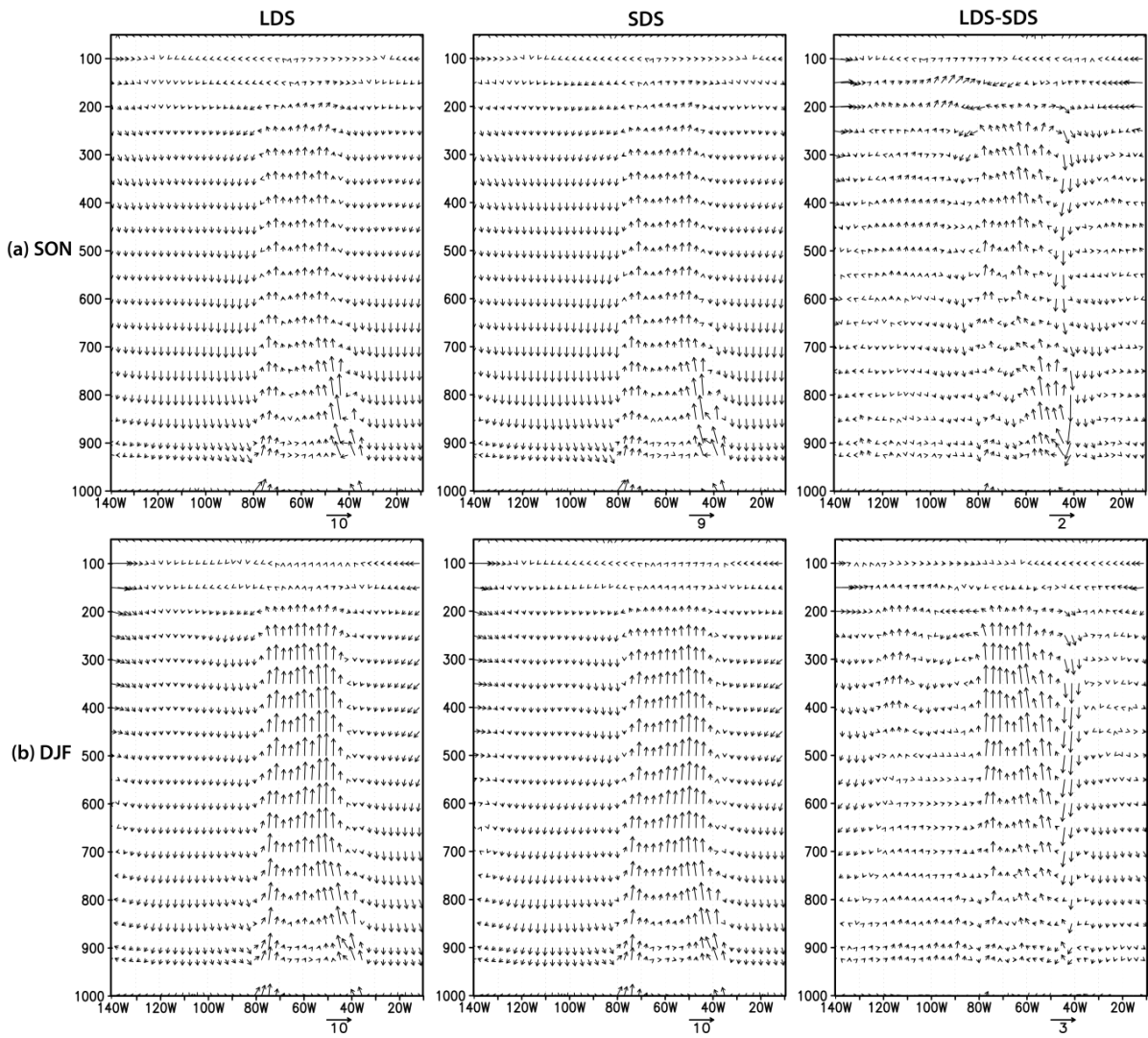


**Figure 11.** Vertical cross-sections for regional zonal divergent circulation over South America during LDS and SDS years, and their difference, for (a) SON, (b) DJF. Vectors are plotted as the divergent meridional wind component and the vertical velocity zonally averaged over the latitudes  $15^{\circ}\text{S}$ - $5^{\circ}\text{S}$ . The vector scale shown in the bottom right corner of each panel is multiplied by  $10^{-4} \text{ hPa s}^{-1}$ .

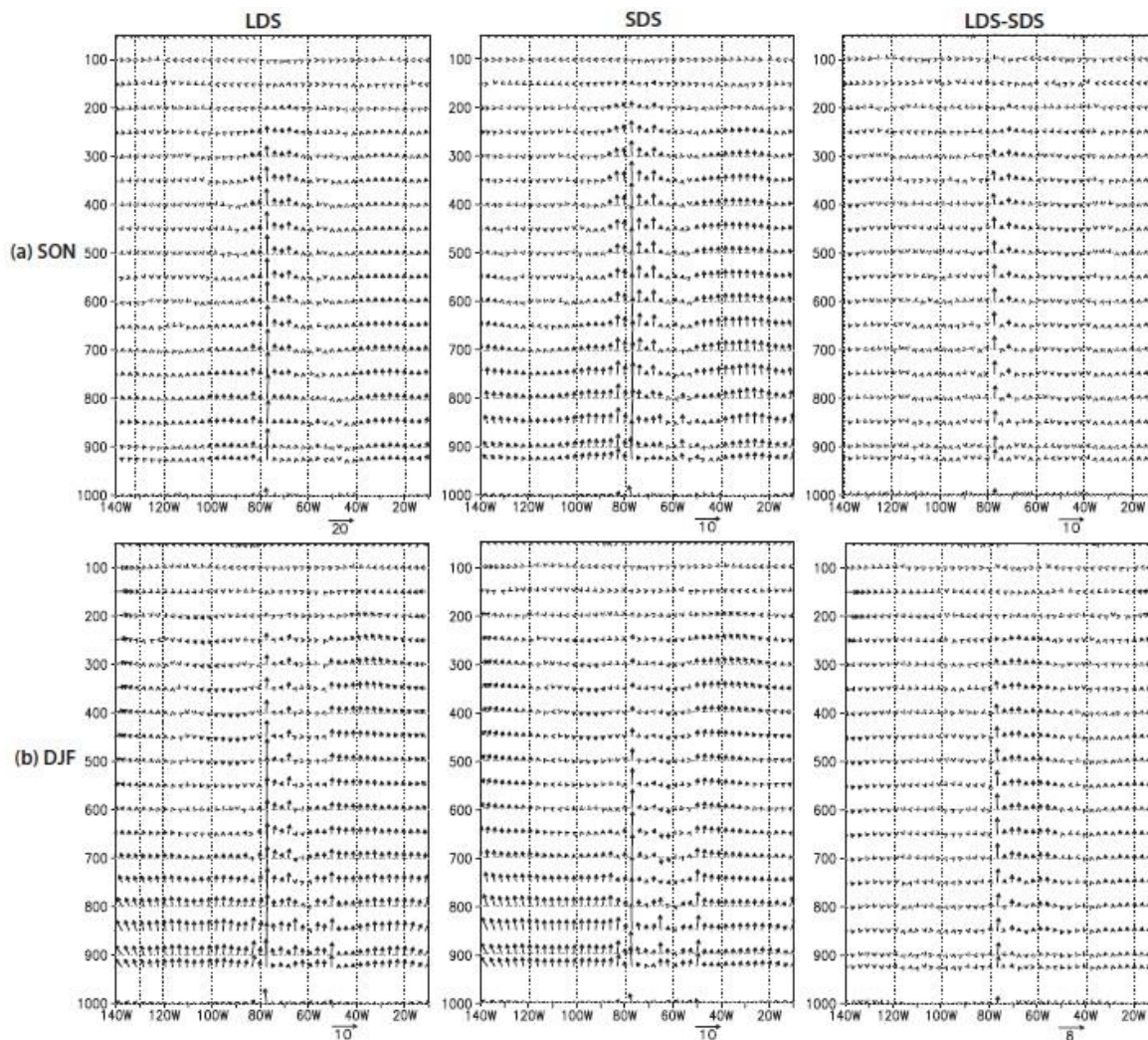


**Figure 12.** Same as Figure 11 but for vertical velocity zonally averaged over latitudes between equator and 10°N.

#### 4. Discussion and Conclusions

A more frequent occurrence of longer dry seasons in the Amazon during the last few decades has been reported by previous studies (Fu et al. 2013; Debortoli et al. 2015) and could be expected under a future warmer climate (Boisier et al. 2015). Recent studies suggest that such a lengthening could be related with regional changes in atmospheric circulation that induce stronger surface moisture convergence over the equatorial Americas and the IAS region, and anomalous subsidence over the Amazon (Arias et al. 2015a). To further explore if a lengthening of the Amazon dry season could relate to changes in atmospheric moisture transport in the Intra-American region, this paper estimates water vapor transport changes in this region during the occurrence of long and short dry seasons in the Amazon, using a semi-Lagrangian model for atmospheric moisture tracking (DRM).

The results suggest that in fact, longer dry seasons in the Amazon are associated with enhanced water vapor transport toward northern South America and the Caribbean and reduced atmospheric moisture in the southern Amazon. Furthermore, our analysis of the regional circulation related to the Hadley and Walker cells indicate that the ascending branches of both cells are enhanced over northern South America while subsidence is strengthened over the southern Amazon basin during its longer dry seasons. This allows us to suggest that regional circulation strengthens during the occurrence of longer dry seasons in the Amazon, in agreement with previous findings (Arias et al. 2015a). However, an important contribution from our study is that the increase of atmospheric moisture over northern South America and the Caribbean is related to

enhanced water vapor transport from oceanic sources, mainly from the tropical north Atlantic (TNA). By contrast, reductions of atmospheric moisture over the southern Amazon are related to inhibited moisture recycling in the region, particularly during the transition period from dry to wet conditions (SON). Figure 13 shows a scheme of the main changes occurred in water vapor transport and recycling during LDS events with respect to climatological conditions. These findings highlight the importance of considering the role of large/regional- scale circulation as well as local-scale processes on atmospheric moisture transport over the Intra-American region.

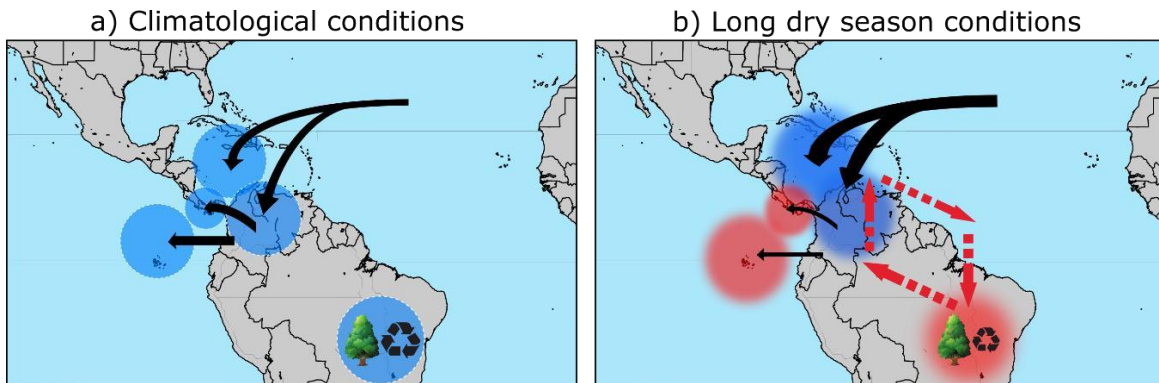


**Figure 13.** Schematics of the main changes of atmospheric moisture transport and recycling over the IAS region during LDS events in the Amazon forest. In a), arrows indicate climatological water vapor transport paths from source to sink regions. Tree and recycling symbols indicate moisture recycling in the Amazon. In b), blue (red) shades indicate increases (reductions) of atmospheric moisture contributions from source to sink regions, as indicated by the arrow. In general, LDS events exhibit enhanced water vapor transport from the Atlantic Ocean toward northern South America and the Caribbean whereas continental contributions from northern South America toward Central America and the eastern Pacific are reduced. In addition, moisture recycling in the Amazon weakens during the LDS events of this forest. Red dotted lines represent the observed changes in the regional Hadley circulation during LDS events, characterized by anomalous subsidence (upward motion) over the southern Amazon (IAS region).

Different authors point out the relevant role of local processes in the Amazon on regional climate in South America (e.g. **Costa and Foley 2000**; **Oyama and Nobre 2003**; **Makarieva and Gorshkov 2006, 2010**; **Costa and Pires 2010**; **Makarieva et al. 2013**). For instance, **Sampaio et al. (2007)** studied the effects of Amazonian deforestation on the regional climate. In their study, the authors simulate land cover maps from a business-as-usual scenario of future deforestation in which rainforest is gradually replaced by degraded pasture or by soybean cropland. Their results show that the most significant changes occur during the Amazon dry season (JJA), where the eastern forest is the most affected region; in particular, their simulations suggest an important increase of near-surface air temperature and decreased evapotranspiration and precipitation in this region. Besides this, **Sampaio et al. (2007)** identify a relevant relationship between precipitation and deforestation, as their study shows an accelerated decrease of rainfall with increasing deforestation for both types of land use conversions. Moreover, **Sampaio (2008)** suggests that a reduction of the Amazon rainforest cover is strongly related to changes in the regional atmospheric circulation pattern.

This study suggests that the occurrence of longer dry seasons in the Amazon is related to stronger regional Walker and Hadley cells, which may influence the ITCZ, strengthening surface moisture convergence over the equatorial region and inducing an increment of atmospheric moisture transport toward northern South America and the Caribbean (Figure 13). However, the reductions of atmospheric moisture over the Amazon observed during such longer dry seasons are not related to changes of contributions from oceanic sources but to reductions of local moisture recycling. Therefore, our results suggest that local surface processes in the Amazon are important both for the local production of atmospheric moisture, and to determine moisture contributions to the Intra-Americas region. In fact, Table 1 suggests that the occurrence of LDS and SDS in this forest are not totally related to the occurrence of larger scale phenomena like El Niño or La Niña events. In addition, our results suggest that during LDS years there is an increase in precipitation over northern South America (Figure 8) and a reduction in the transport of water vapor from northern South America to Central America (calculation not shown, but sketched in Figure 13). This result is in agreement with the reduced

transport from the Magdalena and Orinoco basins to Panamá and Costa Rica when there is an increase in precipitation over northern South America, as found in a previous study that uses the FLEXPART model (**Durán-Quesada et al. 2017**).

To further address the relative role of local processes (represented by vegetation cover) and regional circulation (represented by SSTs in the Atlantic) on the length of the dry season in the Amazon, Figure 14a shows the relationship between LAI anomalies averaged over the southern Amazon, SST anomalies averaged over the TNA, and the occurrence of LDS and SDS events in the Amazon. Our exploratory analysis indicates that LDS (SDS) events are favored when Amazon LAI is reduced (increased) and TNA SSTs increase (reduce) (Figure 14a). In particular, LDSs occur mainly when the Amazon rainforest cover is reduced (negative LAI anomalies), suggesting that local reductions of vegetation cover, such as those related to deforestation, favor the occurrence of longer dry seasons in this forest.

Figures 14b and 14c show total precipitable water composited for the years with LAI anomalies larger (smaller) than the climatological mean plus (minus)  $0.75\sigma$ , respectively. Results indicate that years with negative LAI anomalies (i.e., less vegetation cover) exhibit reduced water vapor over the Amazon, mainly due to changes in moisture supply from local continental sources (not shown). In contrast, increased atmospheric moisture is observed over northern South America and the Caribbean, which is related to enhanced moisture advection from the Atlantic (not shown). The latter resembles findings shown in Figure 6. A similar composite analysis based on TNA SST anomalies indicates that years with warmer conditions in the TNA region relate with enhanced moisture advection from the Atlantic toward northern South America and the Caribbean rather than with moisture reductions in the Amazon (Figures 14d and 14e). The analysis of Figure 14 suggests that both regional circulation associated with ocean-atmosphere interactions and local processes related to vegetation cover are important to determine moisture advection from oceanic sources toward northern South America and the Caribbean. However, local changes in atmospheric moisture supply to the Amazon forest are mainly related to changes in moisture recycling rather than to regional circulation changes, as suggested by the larger anomalies over the southeastern Amazon in the LAI composites (Figures 14b and 14c) compared to the TNA SST composites (Figures 14d and 14e). Further modeling studies are required in order to isolate the relative contributions from both processes (regional vs. local) to the recent lengthening of the dry season in the Amazon.

Finally, it is important to point out that large modifications on the vegetation cover in the Amazon basin have taken place throughout the last 30 years, mainly due to deforestation and land use change related to the expansion of the agricultural and livestock sector (**Fearnside 2005; Davidson et al. 2012**). These processes largely affect vegetation land cover of the region, reducing the extension of the Amazon forest. Moreover, features such as the vegetation type in the region are of high interest for climate regulation. In fact, this feature is one of the leading climate and hydrology modulators in the Amazon, since one of the main sources of atmospheric moisture for this region is the local moisture recycling. As this study highlights, such vegetation cover reductions may contribute to a more frequent occurrence of longer dry seasons in the Amazon, modifying moisture transport patterns not only in the Amazon but also in the entire IAS region.



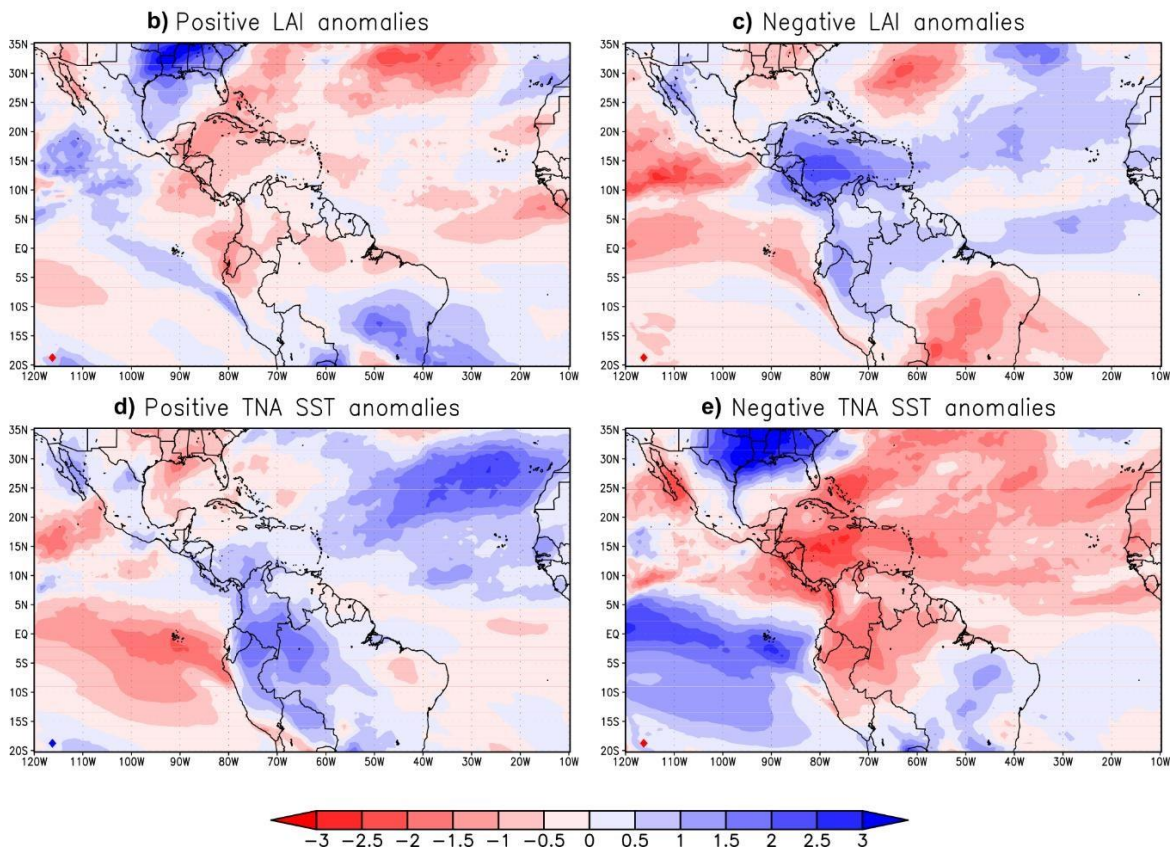
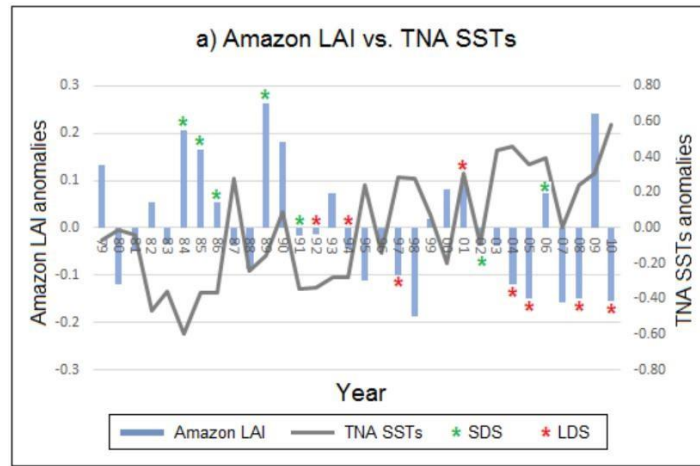


**Figure 14.** a) Annual time series of LAI anomalies averaged over the southern Amazon (5-15°S 40-55°W) (bars) and TNA SST anomalies (5-25°N 30-60°W) (solid line) during the transition period from dry to wet conditions in the Amazon (SON). LDS (SDS) years are indicated by red (green) asterisks. Maps show total precipitable water during the years selected for b) positive LAI anomalies, c) negative LAI anomalies, d) positive TNA SSTs anomalies, and e) negative TNA SSTs anomalies. Values are in mm/day.

### Acknowledgments

This work was supported by “Departamento Administrativo de Ciencia, Tecnología e Innovación de Colombia” (Colciencias) Grant no. 115-660-44588. We acknowledge Rong Fu for her insightful comments and Nathalia Correa-Carmona for providing the data used in Figure 2. A special acknowledgement to John Alejandro Martínez for providing important advises about the DRM model.



## References

- Adler RF, Huffman GJ, Chang , Ferraro R, Xie P, Janowiak J, Rudolf B, Schneider U, Curtis S, Bolvin D, Gruber A, Susskind J, Arkin P (2003) The Version 2 Global Precipitation Climatology Project (GPCP) Monthly Precipitation Analysis (1979-Present). *Journal of Hydrometeorology*, 4, 1147-1167.
- Arias PA, Fu R, Mo K (2012) Changes in monsoon regime over northwestern Mexico in recent decades and its potential causes. *Journal of Climate*, 25, 4258-4274.
- Arias PA, Fu R, Vera C, Rojas M (2015a) A correlated shortening of the North and South American monsoon seasons in the past few decades. *Climate dynamics*, 45(11-12), 3183-3203.
- Arias PA, Martínez JA, Vieira SC (2015b) Moisture sources to the 2010-2012 anomalous wet season in northern South America. *Climate Dynamics*, 45(9-10), 2861-2884.
- Ashouri H, Hsu K, Sorooshian S, Braithwaite DK, Knapp KR, Cecil LD, Nelson BR, Prat OP (2015) PERSIANN-CDR: Daily Precipitation Climate Data Record from Multisatellite Observations for Hydrological and Climate Studies. *Bulletin of the American Meteorological Society*, 96, 69-83.
- Boisier JP, Ciais P, Ducharne A, Guimberteau M (2015) Projected strengthening of Amazonian dry season by constrained climate model simulations. *Nature Climate Change*, 5(7), 656-660.
- Carvalho L, Jones C, Silva AE, Liebmann B, Silva Dias PL (2011) The South American monsoon system and the 1970s climate transition. *International Journal of Climatology*, 31(8), 1248-1256.
- Costa MH, Foley JA (2000) Combined effects of deforestation and doubled atmospheric CO<sub>2</sub> concentrations on the climate of Amazonia. *Journal of Climate*, 13(1), 18-34.
- Costa MH, Pires GF (2010) Effects of Amazon and Central Brazil deforestation scenarios on the duration of the dry season in the arc of deforestation. *International Journal of Climatology*, 30(13), 1970-1979.
- Davidson EA, de Araújo AC, Artaxo P, Balch JK, Brown IF, Bustamante MM, Munger JW (2012) The Amazon basin in transition. *Nature*, 481(7381), 321-328.
- Debortoli NS, Dubreuil V, Funatsu B, Delahaye F, De Oliveira CH, Rodrigues-Filho S, Fetter R (2015) Rainfall patterns in the Southern Amazon: a chronological perspective (1971–2010). *Climatic Change*, 132(2), 251-264.
- Dee DP, Uppala SM, Simmons AJ, Berrisford P, Poli P, Kobayashi S, Bechtold P (2011) The ERA- Interim reanalysis: Configuration and performance of the data assimilation system. *Quarterly Journal of the royal meteorological society*, 137(656), 553-597.
- Dirmeyer PA, Brubaker KL, DelSole T (2009). Import and export of atmospheric water vapor between nations. *Journal of hydrology*, 365(1), 11-22.
- Domínguez F, Kumar P, Liang XZ, Ting M (2006) “Impact of atmospheric moisture storage on precipitation recycling”. *Journal of climate*, 19(8), 1513-1530.
- Drumond A, Marengo J, Ambrizzi T, Nieto R, Moreira L, Gimeno L (2014) The role of the Amazon Basin moisture in the atmospheric branch of the hydrological cycle: a Lagrangian analysis. *Hydrology and Earth System Sciences*, 18, 2577-2598.
- Durán-Quesada AM, Gimeno L, Amador J (2017) Role of moisture transport for Central American precipitation. *Earth System Dynamics*, 8, 147–161.
- Fearnside PM (2005) Deforestation in Brazilian Amazonia: history, rates, and consequences. *Conservation biology*, 19(3), 680-688.

Foley JA, Asner GP, Costa MH, Coe MT, DeFries R, Gibbs HK, Snyder P (2007). Amazonia revealed: forest degradation and loss of ecosystem goods and services in the Amazon Basin. *Frontiers in Ecology and the Environment*, 5(1), 25-32

Fu R, Li W (2004) The influence of the land surface on the transition from dry to wet season in Amazonia. *Theoretical and applied climatology*, 78(1-3), 97-110.

Fu R, Yin L, Li W, Arias PA, Huang L, Myneni RB (2013) "Increased dry-season length over southern Amazonia in recent decades and its implication for future climate projection". *Proceedings of the National Academy of Sciences*, 110(45), 18110-18115.

Goessling H, Reick CH (2013) On the "well-mixed" assumption and numerical 2-D tracing of atmospheric moisture. *Atmospheric Chemistry and Physics*, 13, 5567-5585.

Hoyos I, Domínguez F, Cañón-Barriga J, Martínez JA, Nieto R, Gimeno L, Dirmeyer PA (2017) Moisture origin and transport processes in Colombia, northern South America. *Climate Dynamics*. Pending minor Revisions.

Juárez RIN, Hodnett MG, Fu R, Goulden ML, von Randow C (2007) Control of dry season evapotranspiration over the Amazonian forest as inferred from observations at a southern Amazon forest site. *Journal of Climate*, 20(12), 2827-2839.

Kousky VE (1988) Pentad outgoing longwave radiation climatology for the South American sector. *Revista Brasileira de Meteorologia*, 3(1), 217-231.

Li W, Fu R (2004) Transition of the large-scale atmospheric and land surface conditions from the dry to the wet season over Amazonia as diagnosed by the ECMWF re-analysis. *Journal of Climate*, 17(13), 2637-2651.

Liebmann B, Allured D (2005) Daily precipitation grids for South America. *Bulletin of the American Meteorological Society*, 86(11), 1567.

Liebmann B, Marengo J (2001) Interannual variability of the rainy season and rainfall in the Brazilian Amazon Basin. *Journal of Climate*, 14(22), 4308-4318.

Makarieva AM, Gorshkov VG (2006) Biotic pump of atmospheric moisture as driver of the hydrological cycle on land. *Hydrology and Earth System Sciences Discussions*, 3(4), 2621-2673.

Makarieva AM, Gorshkov VG (2010) The biotic pump: Condensation, atmospheric dynamics and climate. *International Journal of Water*, 5(4), 365-385.

Makarieva AM, Gorshkov VG, Sheil D, Nobre AD, Li BL (2013) Where do winds come from? A new theory on how water vapor condensation influences atmospheric pressure and dynamics. *Atmospheric Chemistry and Physics*, 13(2), 1039-1056.

Marengo JA, Liebmann B, Kousky VE, Filizola NP, Wainer IC (2001) Onset and end of the rainy season in the Brazilian Amazon Basin. *Journal of Climate*, 14(5), 833-852.

Martínez JA, Domínguez F (2014) Sources of Atmospheric Moisture for the La Plata River Basin\*. *Journal of Climate*, 27(17), 6737-6753.

Morton DC, DeFries RS, Shimabukuro YE, Anderson LO, Arai E, del Bon Espirito-Santo F, Morissette J (2006) Cropland expansion changes deforestation dynamics in the southern Brazilian Amazon. *Proceedings of the National Academy of Sciences*, 103(39), 14637-14641.

Oyama MD, Nobre CA (2003) A new climate-vegetation equilibrium state for tropical South America. *Geophysical research letters*, 30(23).

Pathak A, Ghosh S, Martínez JA, Domínguez F, Kumar P (2017). Role of Oceanic and Land Moisture

Sources and Transport in the Seasonal and Inter-annual variability of Summer Monsoon in India. *Journal of Climate*, 30:5, 1839-1859. Online publication date: 23-Feb-2017.

Poveda G, Jaramillo L, Vallejo LF (2014) Seasonal precipitation patterns along pathways of South American low-level jets and aerial rivers. *Water Resources Research*, 50(1), 98-118.

Poveda G, Mesa OJ (2000) On the existence of Lloró (the rainiest locality on earth): enhanced ocean-land-atmosphere interaction by a low-level jet. *Geophysical research letters*, 27(11), 1675-1678.

Salazar LF, Nobre CA (2010) Climate change and thresholds of biome shifts in Amazonia. *Geophysical Research Letters*, 37(17).

Sampaio G (2008) Consequências climáticas da substituição gradual da floresta tropical amazônica por pastagem degradada ou por plantação de soja: um estudo de modelagem. 417 p. INPE-15263-TDI/1346). Tese (Doutorado em Meteorologia)-Instituto Nacional de Pesquisas Espaciais, São José dos Campos.

Sampaio G, Nobre C, Costa MH, Satyamurty P, Soares-Filho BS, Cardoso M (2007) Regional climate change over eastern Amazonia caused by pasture and soybean cropland expansion. *Geophysical Research Letters*, 34(17).

Schellekens J, Calton B, den Heijer K, Dutra E, Sperna Weiland F (2015, April) Opening up a global water resources re-analysis dataset: the earth2Observe tier-1 dataset and portal. In *EGU General Assembly Conference Abstracts* (Vol. 17, p. 9217).

Sierra JP, Arias PA, Vieira SC, Agudelo J (2017) How well do CMIP5 models simulate the low-level jet in western Colombia? *Climate Dynamics*, Under Review.

Soares-Filho BS, Nepstad DC, Curran LM, Cerqueira GC, Garcia RA, Ramos CA, Schlesinger P (2006) Modelling conservation in the Amazon Basin. *Nature* 440: 520-523. *Geophysical Research Letters*, 33, L12704.

Trenberth KE, Fasullo JT, Mackaro J (2011) Atmospheric moisture transports from ocean to land and global energy flows in reanalyses. *Journal of Climate*, 24(18), 4907-4924.

Van der Ent RJ, Tuinenburg OA, Knoche HR, Kunstmann H, Savenije HHG (2013) Should we use a simple or complex model for moisture recycling and atmospheric moisture tracking?. *Hydrology and Earth System Sciences Discussions*, 10 (5), 2013.

Xie P, Arkin PA (1997) Global precipitation: A 17-year monthly analysis based on gauge observations, satellite estimates, and numerical model outputs. *Bulletin of the American Meteorological Society*, 78, 2539 - 2558.

Yin L, Fu R, Zhang YF, Arias PA, Fernando DN, Li W, Bowerman AR (2014) What controls the interannual variation of the wet season onsets over the Amazon?. *Journal of Geophysical Research: Atmospheres*, 119(5), 2314-2328.

Zhang G, Wang Z (2013) Interannual Variability of the Atlantic Hadley Circulation in Boreal Summer and Its Impacts on Tropical Cyclone Activity. *Journal of Climate*, 26, 8529-8544.